



Calculation of Circumferential Stress in Steel Epoxy Sleeve-Reinforced Pipelines Under Internal Pressure



Xinyang Zhang¹, Haonan Liu², Jiaqin Zhang³, Yanke Shi^{1*}, Leige Xu¹

¹ School of Civil Engineering and Communication, North China University of Water Resources and Electric Power, 450045 Zhengzhou, China

² Lan Chengyu Oil-Pipe Branch of Southwest Pipeline Co., Ltd. of PipeChina, 610037 Chengdu, China

³ Dehong Oil and Gas Transmission Branch of National Pipeline Network Group Southwest Oil and Gas Pipeline Co., Ltd., 678499 Dehong, China

* Correspondence: Yanke Shi (shianke@ncwu.edu.cn)

Received: 04-26-2024

Revised: 06-15-2024

Accepted: 06-22-2024

Citation: X. Y. Zhang, H. N. Liu, J. Q. Zhang, Y. K. Shi, and L. G. Xu, "Calculation of circumferential stress in steel epoxy sleeve-reinforced pipelines under internal pressure," *J. Civ. Hydraul. Eng.*, vol. 2, no. 2, pp. 120–130, 2024. <https://doi.org/10.56578/jche020205>.



© 2024 by the author(s). Published by Acadlore Publishing Services Limited, Hong Kong. This article is available for free download and can be reused and cited, provided that the original published version is credited, under the CC BY 4.0 license.

Abstract: To address the lack of clear formulae for calculating the circumferential stress in steel epoxy sleeve-reinforced pipelines under internal pressure, this study constructs a mechanical model based on the specific stress characteristics of these pipelines. Using stress solution methods and deformation compatibility relationships, theoretical formulas for circumferential stress in the pipeline layer, epoxy resin layer, and sleeve layer under internal pressure are derived. The theoretical formulas are validated through numerical simulations using ANSYS software, which includes models with and without flanges. The calculations were performed for common pipelines with outer diameters of 219mm, 660mm, and 1219mm. The results show that the discrepancies between theoretical and numerical solutions of circumferential stress in all layers of both model types are within 10%. Specifically, the circumferential stress in the pipeline layer of the flanged model is lower than that of the non-flanged model and also lower than the theoretical values. The error between the theoretical and numerical solutions for pipelines of different diameters does not exceed 10%, confirming the validity and applicability of the theoretical formulas. This suggests that using the simplified mechanical model for circumferential stress calculations ensures a conservative approach for the structural assessment of pipelines. The formulas provided herein can serve as a reference for the design and evaluation of steel epoxy sleeve-reinforced pipelines under internal pressure.

Keywords: Epoxy sleeve; Pipeline; Circumferential stress; Theoretical solution; Numerical solution

1 Introduction

In recent years, China has increasingly focused on the circulation of strategic resources such as oil and natural gas both domestically and internationally, with pipelines being extensively utilized in oil and gas transportation projects [1, 2]. Due to the instability of the transported media and environmental factors such as corrosion and transportation distance, pipelines are prone to defects like substandard circumferential weld quality, and the circumferential load-bearing capacity of defective sections of pipelines has attracted considerable attention from many scholars [3, 4]. As a non-welding, pressure-bearing repair method that does not require hot work, steel epoxy sleeves have been consistently used in pipeline repair and reinforcement [5–7]. To ensure normal pipeline operation and enhance the circumferential load-bearing capacity at defect locations, it is crucial to clarify the repair and reinforcement effects of epoxy sleeves on pipelines and to master the formulas for calculating circumferential stress in steel epoxy sleeve-reinforced pipelines.

Many scholars have conducted research on the technology of steel epoxy sleeve-repaired pipelines. Zhang et al. [8] discussed the repair principles of steel epoxy sleeve-repaired pipeline technology and its engineering applications and research progress. Jing [9] studied the interfacial bonding performance of steel epoxy sleeve-reinforced pipelines through numerical simulation combined with full-scale pipeline tests. Huo et al. [10] explored the repair effects of steel epoxy sleeves on circumferential seam defects through pipeline tensile tests and finite element simulations. Pang and Dong [11] analyzed the filling process of epoxy resin materials and developed a construction technique for

repairing bent pipes with epoxy sleeves. Yu et al. [12, 13] verified the accuracy of the finite element model through mechanical tests and finite element numerical simulation techniques, and found that epoxy sleeves have a good repair effect on pipelines. Bian et al. [14] conducted mechanical tests to study the axial repair effects of steel epoxy sleeves on pipelines with defects, finding that the axial reinforcement effect of steel epoxy sleeves on defective pipelines is not significant. Shang et al. [15] performed full-scale tensile tests on pipelines repaired with epoxy sleeves, finding that the shear strength between the filling resin and the steel material is very low, and that the axial reinforcement effect of steel epoxy sleeves on pipelines is not significant. Lai et al. [16] tested the mechanical properties of epoxy resin through mechanical experiments and analyzed the repair effects of epoxy sleeve repairs on pipelines. From the above literature, it is known that steel epoxy sleeve repair technology is a good repair method with effective reinforcement effects on pipelines. Some scholars focused on studying the repair effects of steel epoxy sleeves on the circumferential load-bearing capacity of pipelines, for instance, Wang [17] specifically studied the internal pressure experiments of steel epoxy sleeve-reinforced pipelines, comparing experimental data to study the effects of flanges and bolts on the distribution of circumferential stress in pipelines. Cai [18] combined mechanical tests with finite element simulation to study the reinforcement effects of steel epoxy sleeves on large-diameter pipelines under the combined action of internal pressure and bending moments, finding significant reinforcement effects. He [19] used ABAQUS software to establish a finite element model of steel epoxy sleeve-repaired pipelines containing circumferential seam cracks, analyzing the reinforcement mechanism and the repair effects on the ultimate load-bearing capacity of pipelines with circumferential seam cracks under internal pressure and bending moments. Zhao et al. [20] conducted static hydrostatic and cyclic pressure tests on steel epoxy sleeve-repaired pipeline models, and combined with test data, analyzed the repair effects of epoxy sleeves on pipelines, finding significant repair effects on circumferential stress in defective pipelines.

In summary, many scholars have studied the repair effects of steel epoxy sleeves on pipelines with defects under different load conditions through mechanical tests and finite element simulation techniques. However, these two evaluation methods are not direct enough in practical engineering. To provide a quick and effective evaluation method, it is still necessary to clarify the theoretical methods for steel epoxy sleeve-repaired pipelines. Based on the stress characteristics of steel epoxy sleeve-reinforced pipelines, this paper establishes a simplified mechanical model, combines stress solution methods and deformation compatibility relationships to derive the theoretical formulas for circumferential stress in steel epoxy sleeve-reinforced pipelines, and validates the rationality and applicability of the theoretical solution through numerical simulation with ANSYS software. The findings of this study can provide a reference for the repair and reinforcement of pipelines under internal pressure by steel epoxy sleeves.

2 Circumferential Stress Theoretical Derivation for Steel Epoxy Sleeve-Repaired Pipelines Under Internal Pressure

2.1 Simplified Model

In engineering practice, the model of a steel epoxy sleeve-repaired pipeline consists of the pipeline, two steel semi-circular sleeves, epoxy resin material, flanges, and bolts. Under uniformly distributed internal pressure, the contact interfaces between the pipeline layer, resin layer, and sleeve layer are tightly bonded without any slippage. To study the cooperative deformation of the sleeve and the pipeline under internal pressure, the pipeline sleeve repair model is mechanically simplified, mainly ignoring the effects of the flanges and bolts at the ends of the model (see in subgraph (a) of Figure 1). It is assumed that under internal pressure, the geometry of the sleeve-repaired pipeline model is centrally symmetric. Based on this simplification, the theoretical solution for circumferential stress is derived (see in subgraph (b) of Figure 1).

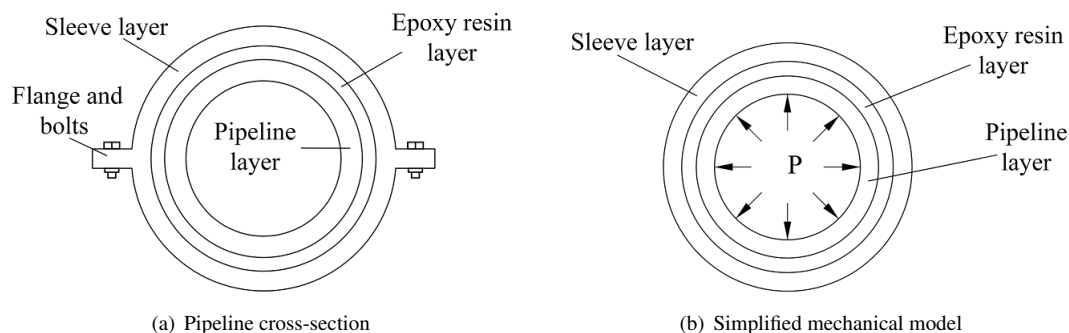


Figure 1. Model simplification diagrams

2.2 Theoretical Derivation Process

The basic assumptions are as follows: (1) The interfaces between the pipeline layer, resin layer, and sleeve layer are tightly bonded and can deform together under internal pressure, without slipping relative to each other; (2) The reinforcing effects of the steel epoxy sleeve's flanges and bolts on the pipeline are ignored, and both the pipeline and sleeve have circular cross-sections; (3) Under the effect of internal pressure, the transfer of forces between the pipeline layer, resin layer, and sleeve layer is completed by the epoxy resin, fulfilling the assumptions of continuity, uniformity, and isotropy of material mechanics, and the deformation of the structure conforms to Hooke's law.

The considered pipeline model is axially symmetric, and under uniformly distributed internal pressure, the stresses and displacements of the steel epoxy sleeve-repaired pipeline are only related to its radius. Based on the theory of inverse solutions in elastic mechanics, the stress of the pipeline can be calculated in polar coordinates, assuming the stress function ϕ only depends on the radial coordinate ρ , given by:

$$\phi = \phi(\rho) \quad (1)$$

In polar coordinates, when body forces are neglected, the expression for the stress components is:

$$\begin{aligned} \sigma_\rho &= \frac{1}{\rho} \frac{\partial \phi}{\partial \rho} + \frac{1}{\rho^2} \frac{\partial^2 \phi}{\partial \varphi^2} \\ \sigma_\varphi &= \frac{\partial^2 \phi}{\partial \rho^2} \\ \tau_{\rho\varphi} &= \tau_{\varphi\rho} = -\frac{\partial}{\partial \rho} \left(\frac{1}{\rho} \frac{\partial \phi}{\partial \varphi} \right) \end{aligned} \quad (2)$$

where: φ is the circumferential coordinate; σ_ρ is the radial stress, Pa; σ_φ is the circumferential stress, Pa; and $\tau_{\rho\varphi}$ and $\tau_{\varphi\rho}$ are the shear stresses, Pa.

By substituting formula (1) into formula (2), the stress components of the pipeline in polar coordinates can be obtained as:

$$\sigma_\rho = \frac{1}{\rho} \frac{d\phi}{d\rho}, \quad \sigma_\varphi = \frac{d^2\phi}{d\rho^2}, \quad \tau_{\rho\varphi} = \tau_{\varphi\rho} = 0 \quad (3)$$

The compatibility equation in polar coordinates can be simplified to:

$$\left(\frac{d^2}{d\rho^2} + \frac{1}{\rho} \frac{d}{d\rho} \right)^2 \phi = 0 \quad (4)$$

Since the compatibility equation in formula (4) is a fourth-order ordinary differential equation, its general solution ϕ can be obtained mathematically as:

$$\phi = A \ln \rho + B\rho^2 \ln \rho + C\rho^2 + D \quad (5)$$

where: A, B, C, D are arbitrary constants.

Substituting formula (5) into formula (3) yields the expression for the stress components of the pipeline, as shown in formula (6):

$$\begin{aligned} \sigma_\rho &= \frac{A}{\rho^2} + B(1 + 2 \ln \rho) + 2C \\ \sigma_\varphi &= -\frac{A}{\rho^2} + B(3 + 2 \ln \rho) + 2C \\ \tau_{\rho\varphi} &= \tau_{\varphi\rho} = 0 \end{aligned} \quad (6)$$

Since the normal stress component depends only on the radial coordinate ρ , and the tangential stress component is zero, this stress state is symmetric about any axial plane and belongs to axial symmetric stress. According to the physical equations, the strain components can be obtained from the stress components, and then the displacement components can be obtained from the strain components according to the geometric equations. The expression for the displacement components is as follows:

$$\begin{aligned} u_\rho &= \frac{1}{E} \left[-(1 + \mu) \frac{A}{\rho} + 2(1 - \mu) B \rho (\ln \rho - 1) + (1 - 3\mu) B \rho + 2(1 - \mu) C \rho \right] + I \cos \varphi + K \sin \varphi \\ u_\varphi &= \frac{4B\rho\varphi}{E} + H\rho - I \sin \varphi + K \cos \varphi \end{aligned} \quad (7)$$

where, u_ρ is the radial displacement component, m; u_φ is the circumferential displacement component, m; E is the elastic modulus of the material, Pa; H, I, K are arbitrary constants.

From the condition of single-valued displacement, it can be deduced that $B=0$. Specifically, within the simplified model, the stress component formulas for the pipeline layer, resin layer, and sleeve layer can be obtained, respectively seen in formulas (8), (9), and (10):

$$\begin{aligned}\sigma_{\rho 1} &= \frac{A_1}{\rho^2} + 2C_1 \\ \sigma_{\varphi 1} &= -\frac{A_1}{\rho^2} + 2C_1 \\ \tau_{\rho\varphi 1} &= 0\end{aligned}\quad (8)$$

where, $\sigma_{\rho 1}$ is the radial stress in the pipeline layer, Pa; $\sigma_{\varphi 1}$ is the circumferential stress in the pipeline layer, Pa; $\tau_{\rho\varphi 1}$ is the shear stress in the pipeline layer, Pa; A_1 and C_1 are arbitrary constants.

$$\begin{aligned}\sigma_{\rho 2} &= \frac{A_2}{\rho^2} + 2C_2 \\ \sigma_{\varphi 2} &= -\frac{A_2}{\rho^2} + 2C_2 \\ \tau_{\rho\varphi 2} &= 0\end{aligned}\quad (9)$$

where, $\sigma_{\rho 2}$ is the radial stress in the resin layer, Pa; $\sigma_{\varphi 2}$ is the circumferential stress in the resin layer, Pa; $\tau_{\rho\varphi 2}$ is the shear stress in the resin layer, Pa; A_2 and C_2 are arbitrary constants.

$$\begin{aligned}\sigma_{\rho 3} &= \frac{A_3}{\rho^2} + 2C_3 \\ \sigma_{\varphi 3} &= -\frac{A_3}{\rho^2} + 2C_3 \\ \tau_{\rho\varphi 3} &= 0\end{aligned}\quad (10)$$

where, $\sigma_{\rho 3}$ is the radial stress in the sleeve layer, Pa; $\sigma_{\varphi 3}$ is the circumferential stress in the sleeve layer, Pa; $\tau_{\rho\varphi 3}$ is the shear stress in the sleeve layer, Pa; A_3 and C_3 are arbitrary constants.

The general solutions for the stress components in the pipeline layer, resin layer, and sleeve layer have been obtained as above. However, due to the presence of unknown parameters, it is still not possible to calculate the stress. The unknown parameters in the formulas need to be solved according to displacement and stress boundary conditions. Assume the uniformly distributed internal pressure load on the pipeline is P , with no shear stress, and zero stress on the outer wall. The expressions for the displacement in the thickness direction of the pipeline layer, resin layer, and sleeve layer can be obtained by substituting formulas (8) through (10) into formula (7) and then simplifying the transformation as shown in formula (11).

$$\begin{aligned}u_{\rho 1} &= \frac{1-\mu_1^2}{E_1} \left[-\frac{A_1}{(1-\mu_1)\rho} + 2C_1\rho \frac{1-2\mu_1}{1-\mu_1} \right] \\ u_{\rho 2} &= \frac{1-\mu_2^2}{E_2} \left[-\frac{A_2}{(1-\mu_2)\rho} + 2C_2\rho \frac{1-2\mu_2}{1-\mu_2} \right] \\ u_{\rho 3} &= \frac{1-\mu_3^2}{E_3} \left[-\frac{A_3}{(1-\mu_3)\rho} + 2C_3\rho \frac{1-2\mu_3}{1-\mu_3} \right]\end{aligned}\quad (11)$$

where, $u_{\rho 1}$ is the radial displacement component of the pipeline layer, m; $u_{\rho 2}$ is the radial displacement component of the resin layer, m; $u_{\rho 3}$ is the radial displacement component of the sleeve layer, m; μ_1 is the Poisson's ratio of the pipeline material, dimensionless; μ_2 is the Poisson's ratio of the resin material, dimensionless; μ_3 is the Poisson's ratio of the sleeve material, dimensionless.

Due to the symmetry of both the structure and the forces acting on the pipeline, and the close contact between the pipeline layer, resin layer, and sleeve layer, continuity of deformation ensures that the displacement boundary conditions and stress boundary conditions at the interfaces between layers are consistent. Under uniformly distributed internal pressure, the stress conditions of the pipeline layer, resin layer, and sleeve layer are illustrated in Figure 2.

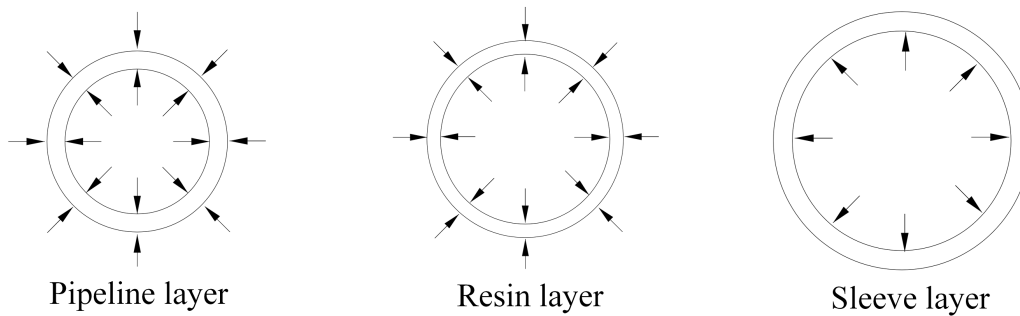


Figure 2. Force diagram of each level model

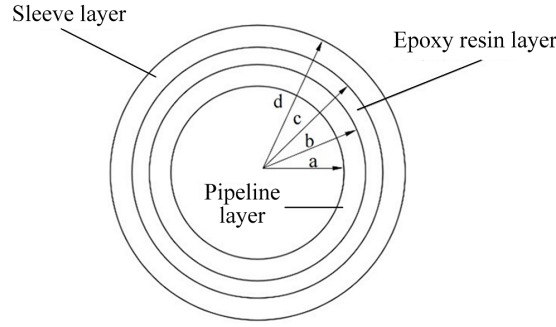


Figure 3. Radius diagram of each level

The distances from the inner and outer walls of the pipeline to the axis are set as a and b , respectively, and the distances from the inner and outer walls of the sleeve to the axis are set as c and d , as shown in Figure 3. Considering the stress boundary conditions and displacement boundary conditions, a matrix equation can be obtained as shown in formula (12).

$$\begin{pmatrix} \frac{1}{a^2} & 0 & 0 & 2 & 0 & 0 \\ 0 & 0 & \frac{1}{d^2} & 0 & 0 & 2 \\ \frac{1}{b^2} & -\frac{1}{b^2} & 0 & 2 & -2 & 0 \\ 0 & \frac{1}{c^2} & -\frac{1}{c^2} & 0 & 2 & -2 \\ 0 & \frac{1+\mu_2}{E_2 b} & 0 & \frac{2(1+\mu_1)(-2\mu_1 b^2 + a^2 + b^2)}{E_1 b} & -\frac{2b(-2\mu_2^2 - \mu_2 + 1)}{E_2} & 0 \\ 0 & -\frac{1+\mu_2}{E_2 c} & \frac{1+\mu_3}{E_3 c} & 0 & \frac{2c(-2\mu_2^2 - \mu_2 + 1)}{E_2} & -\frac{2c(-2\mu_3^2 - \mu_3 + 1)}{E_3} \end{pmatrix} \begin{pmatrix} A_1 \\ A_2 \\ A_3 \\ C_1 \\ C_2 \\ C_3 \end{pmatrix} = \begin{pmatrix} -P \\ 0 \\ 0 \\ 0 \\ -\frac{a^2 P(1+\mu_1)}{E_1 b} \\ 0 \end{pmatrix} \quad (12)$$

Due to the multiple parameters in the matrix equation, this paper solved it using MATLAB. First, the model dimensions and parameters were inputted, then the unknown constant parameters were calculated, and by substituting these into formulas (8) through (10), the theoretical values of the circumferential stress can be obtained.

3 Finite Element Analysis Validation of Theoretical Formulas

3.1 Model Parameters

To verify the rationality and applicability of the theoretical formulas for circumferential stress derived from the simplified model, ANSYS finite element software was used to perform numerical simulations on the epoxy sleeve-repaired pipeline model. Since flanges and bolts are present at the ends of the steel epoxy sleeves in engineering practice, their effects on the epoxy sleeve-repaired pipeline were neglected from a mechanical equivalence perspective during theoretical derivation, considering the overall structure as an ideal cylindrical model. This simplification, which omits flanges and bolts, is conservative for structural calculations and allows for validation of the theoretical circumferential stress formulas using both a flangeless sleeve-repaired pipeline model and a flanged sleeve-repaired pipeline model. The flangeless sleeve-repaired pipeline model has a pipeline layer length of 6m, a resin layer length of 3m, and a sleeve layer length of 3m (see Table 1). The flanged sleeve-repaired pipeline model has one side flange strip total length of 3m, height 0.0946m, minimum width 0.107m, and maximum width 0.109m, with other dimensions and parameters consistent with the flangeless model.

Table 1. Material parameters of pipe model repaired by flangeless sleeve

Material	Length/m	Inner Diameter/m	Outer Diameter/m	Wall Thickness/m	Elastic Modulus/Pa	Poisson's Ratio	Pipe Material
Pipeline layer	6	0.9854	1.0160	0.0153	2.07×10^{11}	0.3	x70
Resin layer	3	1.0160	1.0360	0.0100	3.0×10^9	0.3	/
Sleeve layer	3	1.0360	1.0860	0.0250	2.07×10^{11}	0.3	x70

3.2 Finite Element Model Establishment

Based on the material parameters and model dimensions of the pipeline, epoxy resin, and sleeve, the flangeless steel epoxy sleeve-repaired pipeline model and the flanged steel epoxy sleeve-repaired pipeline model were established

using solid185 solid elements. After discretization and mesh division, the hexahedral cell size for both the flangeless sleeve model and the flanged sleeve model is 0.02m, with the number of mesh cells being 129,000 (node count 186,560) and 142,800 (node count 205,392), respectively. To eliminate the influence of mesh size on the simulation results, a comparative analysis with mesh sizes of 0.01m and 0.04m was conducted, showing that the relative error in circumferential stress did not exceed 5%, indicating that the chosen mesh size and number can meet the accuracy requirements of the simulation calculations. Subsequently, both models were subjected to a uniformly distributed pressure of 10 MPa directed radially towards the inner wall of the pipeline, along with axial constraints applied at the ends of the pipeline and constraints on the upper and lower nodes of the inner and outer walls of the circular cross-sections in the x-axis direction, and left and right nodes in the y-axis direction. The sleeve-repaired pipeline model is shown in Figure 4.

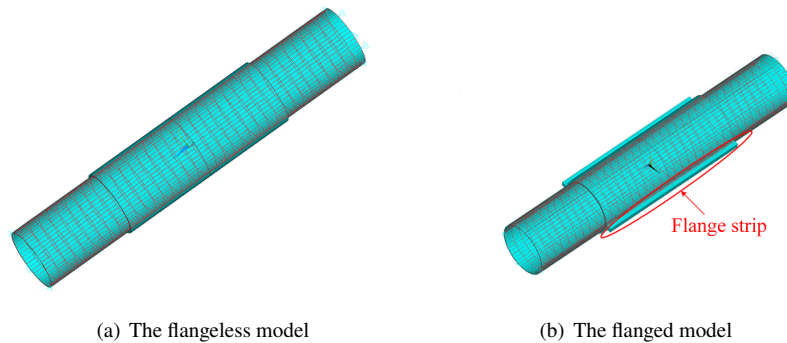


Figure 4. Diagrams of Two models

3.3 Finite Element Analysis Results

The distribution of circumferential stress in the pipeline layer of the flangeless sleeve-repaired pipeline model is shown in subgraph (a) of Figure 5. The circumferential stress in the pipeline reaches 334 MPa in sections not covered by the sleeve and exhibits stress concentration at the edges of the sleeve coverage, whereas in areas far from the edges under sleeve coverage, the circumferential stress is uniformly distributed and only 128 MPa. The distribution of circumferential stress in the pipeline layer of the flanged sleeve-repaired pipeline model is shown in subgraph (b) of Figure 5, where the circumferential stress in the sections not covered by the sleeve is 367 MPa. Similar to the flangeless model, stress concentration occurs at the sleeve edges, while in areas far from the edges under sleeve coverage, the circumferential stress is uniformly distributed and only 124 MPa. Whether in the flanged or flangeless model, the circumferential stress in the pipeline layer is significantly reduced in the sleeve-covered sections. This is consistent with the findings of full-scale internal pressure experiments on steel epoxy sleeve-reinforced pipelines reported in literature [17], and pressure fluctuation tests using steel epoxy sleeves to repair circumferential stress in pipelines as mentioned in literature [20], confirming that using epoxy sleeves for pipeline repair and reinforcement is effective.

The distribution of circumferential stress in the resin layer of the flangeless sleeve-repaired pipeline model is shown in subgraph (a) of Figure 6. The circumferential stress in the resin layer is uniformly distributed away from the sleeve edges and only 0.553 MPa, with the maximum stress concentration at the sleeve edges being 1.33 MPa. The distribution of circumferential stress in the resin layer of the flanged sleeve-repaired pipeline model is shown in subgraph (b) of Figure 6. The circumferential stress distribution in the flanged model's resin layer is similar to that in the flangeless model, but the circumferential stress away from the sleeve edges is 0.886 MPa, with the maximum stress at the sleeve edges being 4.17 MPa.

As shown in subgraph (a) of Figure 7, the distribution of circumferential stress in the sleeve layer of the flangeless model is essentially consistent with that in the resin layer, with the circumferential stress being 111 MPa in regions far from the edges and a maximum of 165 MPa at the edges. According to subgraph (b) of Figure 7, the circumferential stress distribution on the non-flange side of the flanged model is uniform at 98.5 MPa, with stress concentration occurring at the edges where the maximum circumferential stress reaches 182 MPa, while the circumferential stress on the flange side is uniformly distributed at only 6.51 MPa. Based on the finite element analysis results, the presence of the flange in the model significantly affects the areas close to the flange, altering the local constraints at the flange, thereby reducing the circumferential stress on the flange side. This indicates that omitting the flange and bolts in the simplification is safer for the overall structure.

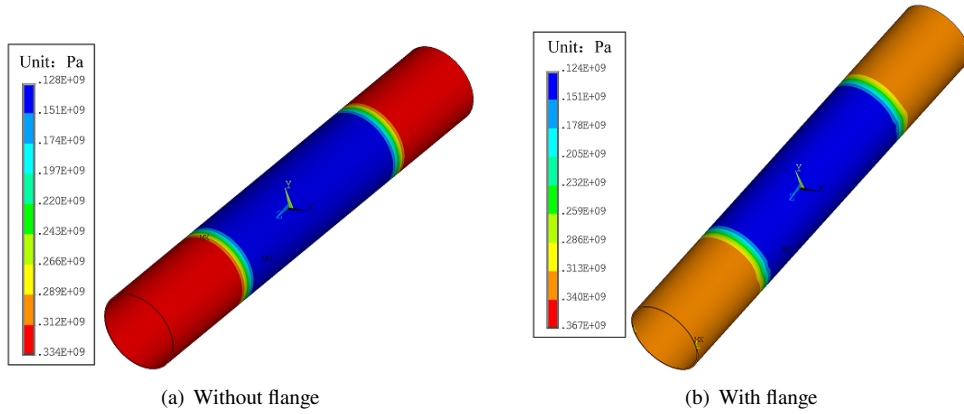


Figure 5. Circumferential stress cloud diagram of pipeline layer

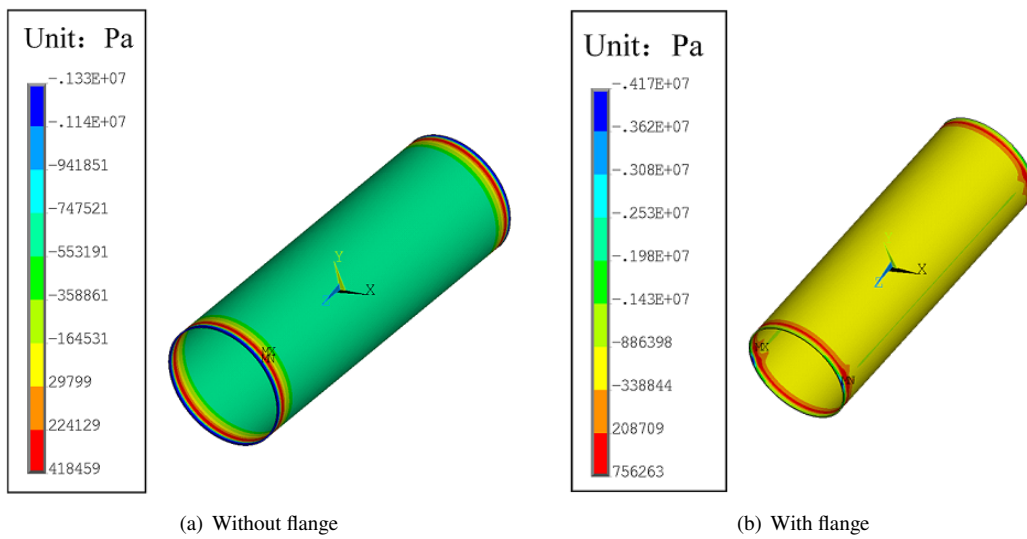


Figure 6. Circumferential stress nephogram of resin layer

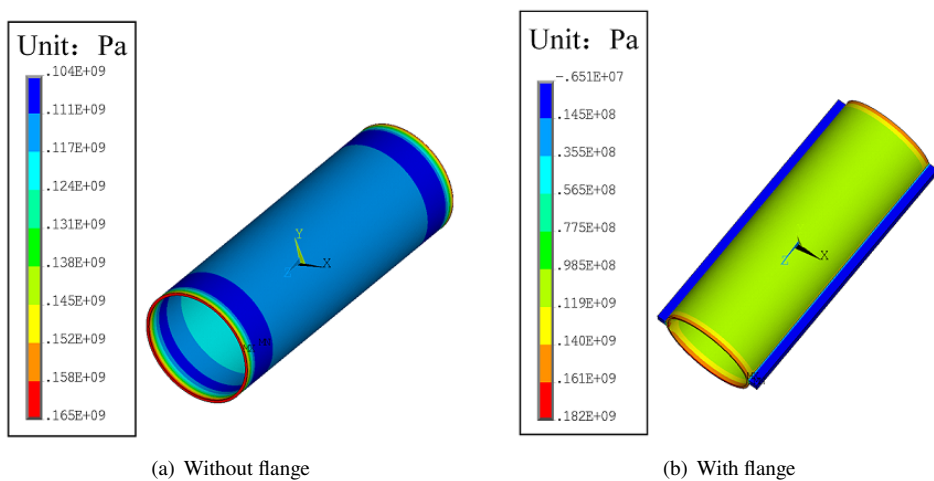


Figure 7. Circumferential stress nephogram of sleeve layer

3.4 Comparison and Analysis of Theoretical and Numerical Solutions

Based on the finite element simulation results, it is evident that the circumferential stress on the flange side of the flanged model is relatively low, indicating that the circumferential stress in the flanged model is primarily controlled

by the non-flange side. Therefore, it is important to focus on analyzing the differences between the numerical solutions of the circumferential stress on the non-flange side of the flanged model and the flangeless model and their corresponding theoretical solutions. To adhere to the principle of single variable analysis, a line was selected along the mid-wall thickness at the position corresponding to the non-flange side of the flanged model, and nodes along this line were extracted to obtain the corresponding circumferential stress values, which were then compared with the theoretical solutions.

From the comparison of the theoretical and numerical solutions of the circumferential stress in the pipeline layer (Table 2), it can be observed that the error between the theoretical and numerical solutions of the circumferential stress in the flangeless model's pipeline layer is very small, with the maximum error due to changes in radius being only 0.6%. The error between the theoretical and numerical solutions of the circumferential stress on the non-flange side of the flanged model is also small, with the maximum error being 1.3%. The comparison shows that the error between the theoretical and numerical solutions of the circumferential stress in the pipeline layer is within 2%. Furthermore, the numerical solutions of the circumferential stress on the flange side of the flanged model and the flangeless model are both less than the theoretical solutions. This indicates that the theoretical formulas for circumferential stress derived from the simplified mechanical model provide a conservative basis for the structural verification of pipelines.

Table 2. Comparison of circumferential stress of pipeline layer

Radius /m	Theoretical Value of Circumferential Stress /MPa	Circumferential Stress on Non-Flange Side /MPa	Error with Theoretical Solution	Circumferential Stress without Flange /MPa	Error with Theoretical Solution
0.4927	133.70	132	-1.3%	132.95	-0.6%
0.4965	132.61	131.69	0.7%	132.65	0.3%
0.5004	131.51	130.92	-0.4%	131.93	0.3%
0.5042	130.46	130.18	-0.2%	131.22	0.6%
0.5080	129.44	129	-0.3%	130.11	0.5%

Table 3 provides a comparison and analysis of the theoretical and numerical solutions for the circumferential stress in the resin layer. As the wall thickness of the epoxy resin layer changes, the error between the theoretical and numerical solutions for the circumferential stress in the flangeless model's resin layer is a maximum of only 3%. For the non-flange side of the resin layer in the flanged model, the error between the theoretical and numerical solutions is also small, with the maximum error being 7%. The comparison indicates that although the presence of the flange in the flanged model has a small impact on the local stress distribution, it also demonstrates that the derived theoretical formulas are reasonable.

Table 3. Comparison of circumferential stress of resin layer

Radius /m	Theoretical Value of Circumferential Stress /MPa	Circumferential Stress on Non-Flange Side /MPa	Error with Theoretical Solution	Circumferential Stress without Flange /MPa	Error with Theoretical Solution
0.508	-0.54718	-0.58560	7%	-0.56416	3%
0.510	-0.56749	-0.59790	5.4%	-0.57740	1.7%
0.512	-0.58756	-0.61020	3.9%	-0.59061	0.5%
0.514	-0.60740	-0.62249	2.5%	-0.60384	-0.6%
0.516	-0.62702	-0.63478	1.2%	-0.61706	-1%
0.518	-0.64640	-0.64708	0.1%	-0.63029	-2.5%

According to the comparison of the theoretical and numerical solutions for the circumferential stress in the sleeve layer (Table 4), the error between the theoretical and numerical solutions for the flangeless model's sleeve layer is very small, with the maximum error caused by changes in the sleeve layer's wall thickness being only 0.4%. The error between the theoretical and numerical solutions for the non-flange side of the sleeve layer in the flanged model is also small, with the maximum error being 1.5%. Overall, the theoretical solutions for circumferential stress derived from the simplified model are consistent with the numerical solutions for the flangeless model. Finite element analysis, which discretizes a continuous elastic body into a finite number of elements and calculates stress and strain through the internal forces of these elements, provides approximate results, while the theoretical formulas provide exact solutions. The small discrepancies between these solutions are reasonable and highlight the advantage of finite element analysis widely used across various fields. The error between the theoretical solutions derived from the simplified model and the numerical solutions for the circumferential stress in the flanged model does not exceed

10%, indicating that the flanged model is not an ideal cylindrical structure. The presence of the flange can alter local constraints to some extent, having a minor impact on local stress distributions. The comparative analysis of the numerical and theoretical solutions for the circumferential stresses in the pipeline layer, resin layer, and sleeve layer shows that the idea of simplifying the sleeve-repaired pipeline model into an ideal cylindrical structure by ignoring flanges and bolts is reasonable. The circumferential stress calculation formulas derived from the simplified mechanical model have significant reference value.

Table 4. Comparison of circumferential stress of sleeve layer

Radius /m	Theoretical Value of Circumferential Stress /MPa	Circumferential Stress on Non-Flange Side /MPa	Error with Theoretical Solution	Circumferential Stress without Flange /MPa	Error with Theoretical Solution
0.518	119.70	119.4	-0.3%	119.19	-0.4%
0.521	118.98	118.93	-0.04%	118.58	-0.3%
0.524	118.28	118.46	0.2%	117.98	-0.3%
0.527	117.58	117.98	0.3%	117.37	-0.2%
0.530	116.90	117.51	0.5%	116.77	-0.1%
0.533	116.22	117.04	0.7%	116.16	-0.05%
0.536	115.56	116.57	0.9%	115.55	-0.01%
0.539	114.91	116.09	1%	114.95	0.03%
0.542	114.27	115.62	1.2%	114.34	0.06%
0.543	114.06	115.74	1.5%	114.49	0.4%

3.5 Validation for Pipelines of Different Diameters

Table 5. Parameters of pipelines with different diameters

Diameter/mm	Material	Length/m	Inner Diameter/m	Outer Diameter/m	Wall Thickness/m	Elastic Modulus/Pa	Poisson's Ratio
219	Pipeline layer	6	0.2054	0.2190	0.0068	2.10×10^{11}	0.3
	Resin layer	3	0.2190	0.2214	0.0012	3.00×10^9	0.3
	Sleeve layer	3	0.2214	0.2390	0.0088	2.10×10^{11}	0.3
660	Pipeline layer	6	0.6362	0.6600	0.0119	2.10×10^{11}	0.3
	Resin layer	3	0.6600	0.6680	0.0040	3.00×10^9	0.3
	Sleeve layer	3	0.6680	0.7080	0.0200	2.10×10^{11}	0.3
1219	Pipeline layer	6	1.1822	1.2190	0.0184	2.10×10^{11}	0.3
	Resin layer	3	1.2190	1.2470	0.0140	3.00×10^9	0.3
	Sleeve layer	3	1.2470	1.3070	0.0300	2.10×10^{11}	0.3

Table 6. Comparison of theoretical and numerical solutions for circumferential stress in pipelines of different diameters

Material	Diameter 219mm			Diameter 660mm			Diameter 1219mm		
	Theoretical Solution /MPa	Numerical Solution /MPa	Error	Theoretical Solution /MPa	Numerical Solution /MPa	Error	Theoretical Solution /MPa	Numerical Solution /MPa	Error
Pipeline layer	71.03	70.98	0.07%	106.96	106.94	0.02%	132.43	132.44	0.07%
Resin layer	-1.1382	-1.1384	0.02%	-0.9881	-0.9884	0.03%	-0.6041	-0.6037	0.07%
Sleeve layer	61.90	61.88	0.03%	96.15	96.18	0.03%	116.05	116.03	0.02%

To verify whether the formulas for calculating the circumferential stress in the pipeline layer, resin layer, and sleeve layer are applicable to pipelines of different diameters, calculations were conducted for three common pipelines with outer diameters of 219mm, 660mm, and 1219mm, as shown in Table 5. The theoretical solutions for the circumferential stress in the middle position of the pipeline layer, resin layer, and sleeve layer (along the thickness direction) under a uniform internal pressure of 10MPa were derived using the developed formulas. Subsequent simulations were carried out for these three different diameter pipeline models, calculating the numerical solutions for circumferential stress at the middle positions of each part, and comparing these with the theoretical solutions. According to Table 6, the error between the theoretical and numerical solutions for the circumferential stress under a

10MPa uniform internal pressure for the three different diameter pipelines is within 10%. The results indicate that, without affecting the mechanical simplification of the pipeline model and under the assumption that basic conditions are met, the derived theoretical formulas can be used to calculate the circumferential stress in sleeve-repaired pipeline models.

4 Conclusions

(1) Based on the stress characteristics of the steel epoxy sleeve-repaired pipeline model under internal pressure, a corresponding simplified mechanical model was established. Theoretical formulas for calculating the circumferential stress in the pipeline layer, resin layer, and sleeve layer of the steel epoxy sleeve-repaired pipeline model under internal pressure were derived, and are applicable for calculating the circumferential stress in steel epoxy sleeve-repaired pipelines under internal pressure.

(2) The numerical analysis results for the circumferential stress in the pipeline layer, resin layer, and sleeve layer of the flanged and flangeless models show that steel epoxy sleeves have a good effect on pipeline repair and reinforcement, consistent with related conclusions from mechanical experiments reported in the literature.

(3) The comparative analysis of the theoretical and numerical solutions for the circumferential stress in the pipeline layer, resin layer, and sleeve layer shows that the error between the theoretical and numerical solutions for the circumferential stress in both models is within 10%. In the pipeline layer, the numerical solutions for circumferential stress on the flange side of the flanged model and the flangeless model are both less than the theoretical solutions, confirming the reasonableness of the circumferential stress calculation formulas and indicating that the theoretical formulas derived from the simplified mechanical model provide a conservative basis for the structural verification of pipelines.

(4) The comparison and analysis of the theoretical and numerical solutions for the circumferential stress in pipelines with outer diameters of 219mm, 660mm, and 1219mm show that the errors between the theoretical solutions calculated using the circumferential stress formulas and the finite element analysis numerical solutions do not exceed 10%, demonstrating the good applicability of the derived circumferential stress solution formulas to common pipelines. In practical engineering, without affecting the mechanical simplification of the pipeline model and while satisfying basic assumption conditions, the derived theoretical formulas for circumferential stress can be appropriately used to calculate solutions for the sleeve-repaired pipeline model.

Data Availability

The data used to support the findings of this study are available from the corresponding author upon request.

Conflicts of Interest

The authors declare that they have no conflicts of interest.

References

- [1] H. Yang, F. X. Wang, T. Zhong, W. B. Xuan, and Z. Q. Lei, "Strain-based applicability evaluation of girth welds on high-grade steel pipeline," *China Pet. Mach.*, vol. 50, no. 5, pp. 150–156, 2022. <https://doi.org/10.16082/j.cnki.issn.1001-4578.2022.05.020>
- [2] H. W. Tao, C. Yang, X. G. Liu, X. Y. Guo, and S. M. Zhang, "Research on sealing method of flexible sleeve for oil and gas pipeline," *China Pet. Mach.*, vol. 50, no. 11, pp. 111–118, 2022. <https://doi.org/10.16082/j.cnki.issn.1001-4578.2022.11.016>
- [3] P. H. Chan, K. Y. Tshai, M. Johnson, and S. Li, "The flexural properties of composite repaired pipeline: Numerical simulation and experimental validation," *Compos. Struct.*, vol. 133, pp. 312–321, 2015. <https://doi.org/10.1016/j.compstruct.2015.07.066>
- [4] L. L. Mathias, D. F. Sarzosa, and C. Ruggieri, "Effects of specimen geometry and loading mode on crack growth resistance curves of a high-strength pipeline girth weld," *Int. J. Press. Vessels Pip.*, vol. 111, pp. 106–119, 2013. <https://doi.org/10.1016/j.ijpvp.2013.06.003>
- [5] W. Y. Wand, Z. Q. Cheng, Y. Zhang, and J. F. Lu, "Numerical simulation of filling process of epoxy resin steel sleeve," *J. Sichuan Univ. Sci. Eng. (Nat. Sci. Ed.)*, vol. 30, no. 6, pp. 18–22, 2017. <https://doi.org/10.11863/j.suse.2017.06.04>
- [6] DNV GL, Loughborough, UK, "Evolution of epoxy sleeve pipeline repair technology," *Pipelines Int.*, vol. 2015, no. 23, pp. 50–52, 2015.
- [7] G. Q. Ren, J. M. Zhang, X. P. He, P. Wang, G. F. Wang, and H. Zhang, "Comparison and analysis of relevant standards for repairing defects of oil and gas long distance pipeline with steel epoxy sleeve," *Welded Pipe Tube*, vol. 46, no. 2, pp. 54–59, 2023. <https://doi.org/10.19291/j.cnki.1001-3938.2023.02.009>

- [8] Z. Y. Zhang, R. Jia, Y. Ji, and J. Xie, "Discussion on the application of steel epoxy sleeve repair technology in long-distance pipeline engineering," *Total Corros. Control*, vol. 37, no. 9, pp. 52–54, 2023. <https://doi.org/10.13726/j.cnki.11-2706/tq.2023.09.052.03>
- [9] D. Y. Jing, "Analysis of interface performance and reinforcement effect of steel epoxy sleeve reinforcement pipeline," Master's thesis, Southwest University of Science and Technology, 2023. <https://doi.org/10.27415/d.cnki.gxngc.2023.000557>
- [10] X. T. Huo, H. F. Lei, P. J. Jia, F. P. Yang, H. Yao, Y. Liu, and C. J. Jiang, "Discussion on epoxy sleeve repair effect verification technology for girth weld defects of large-diameter trunk pipeline," *Inner Mongolia Petrochem. Ind.*, vol. 48, no. 05, pp. 68–73, 2022.
- [11] P. Pang and S. H. Dong, "Development of steel socket epoxy reinforcement deflection repair technology and application research," *Pipeline Tech. Equip.*, vol. 2019, no. 4, pp. 44–48, 2019. <https://doi.org/10.3969/j.issn.1004-9614.2019.04.012>
- [12] D. L. Yu, C. Yang, D. R. Wu, Y. Jiang, and Y. C. Fang, "Study on repairing and reinforcing effect of steel epoxy sleeve on girth weld defects," *China Pet. Mach.*, vol. 50, no. 6, pp. 121–127, 2022. <https://doi.org/10.16082/j.cnki.issn.1001-4578.2022.06.018>
- [13] D. L. Yu, C. Yang, D. R. Wu, A. L. Wang, H. Huang, B. Jia, and Y. Zhang, "Reinforcement test of epoxy-filled steel sleeves for girth weld defects of X80 pipelines," *Oil Gas Storage Transp.*, vol. 40, no. 9, pp. 997–1007, 2021. <https://doi.org/10.6047/j.issn.1000-8241.2021.09.005>
- [14] Y. H. Bian, H. P. Hu, D. G. Zhang, G. J. Diao, J. F. Lu, Z. K. Zhao, W. Sun, and M. J. Zhang, "Study on axial repair effect of epoxy-filled steel sleeve," *Welded Pipe Tube*, vol. 45, no. 3, pp. 36–40, 2022. <https://doi.org/10.19291/j.cnki.1001-3938.2022.03.007>
- [15] F. Shang, Y. H. Huang, Y. J. Wu, and X. L. Wu, "Analysis of axial repair effect of girth weld defects in steel epoxy sleeve," *Tech. Superv. Pet. Ind. J. Agency*, vol. 38, no. 4, pp. 21–23, 2022. <https://doi.org/10.3969/j.issn.1004-1346.2022.04.005>
- [16] S. C. Lai, S. L. Fu, Y. M. Lin, G. Y. Li, and L. Zhong, "Structure and performance of epoxy sleeve pipe reinforcement and repair material," *Mod. Plast. Process. Appl.*, vol. 33, no. 3, pp. 29–31, 2021. <https://doi.org/10.19690/j.issn1004-3055.20200150>
- [17] Z. Y. Wang, "Mechanical properties of steel epoxy sleeve reinforced X80 pipe under internal pressure," Master's thesis, Southwest University of Science and Technology, 2022. <https://doi.org/10.27415/d.cnki.gxngc.2022.000376>
- [18] Z. J. Cai, "Study of repair and reinforcement on X80 pipeline with girth weld flaw with steel epoxy sleeve," Master's thesis, Southwest University of Science and Technology, 2022. <https://doi.org/10.27415/d.cnki.gxngc.2022.000044>
- [19] Y. He, "Study on the ultimate load carrying capacity of steel epoxy sleeve repair for pipes containing ring weld cracks," Master's thesis, Southwest University of Science and Technology, 2023. <https://doi.org/10.27415/d.cnki.gxngc.2023.000927>
- [20] X. F. Zhao, Y. H. Duan, and Y. Jiang, "Study on the applicability of epoxy sleeve for repairing defects of girth welds," *Mod. Chem. Res.*, vol. 67, no. 14, pp. 150–153, 2020. <https://doi.org/10.3969/j.issn.1672-8114.2020.14.068>